galaxies

MDPI

Article

Cryogenic Facility for Prototyping ET-LF Payloads Using Conductive Cooling

Marco Ricci [1,2,*], Eugenio Benedetti [1], Angelo Cruciani [1], Van Long Hoang [1,2], Benedetta Kalemi [1,2], Luca Naticchioni [1,2], Marco Orsini [1,2], Stefano Pirro [3], Paola Puppo [1,2], Piero Rapagnani [1,2], Fulvio Ricci [1], Emanuele Tofani [1] and Ettore Majorana [1,2]

[1] INFN Sezione di Roma, P.le A. Moro 2, 00185 Roma, Italy; eugenio.benedetti@roma1.infn.it (E.B.); angelo.cruciani@roma1.infn.it (A.C.); vanlong.hoang@uniroma1.it (V.L.H.); benedetta.kalemi@uniroma1.it (B.K.); luca.naticchioni@roma1.infn.it (L.N.); marco.orsini@uniroma1.it (M.O.); paola.puppo@roma1.infn.it (P.P.); piero.rapagnani@roma1.infn.it (P.R.); fulvio.ricci@roma1.infn.it (F.R.); emanuele.tofani@unicampania.it (E.T.); ettore.majorana@roma1.infn.it (E.M.)
[2] Department of Physics, Sapienza Università di Roma, P.le A. Moro 2, 00185 Roma, Italy
[3] INFN Laboratori Nazionali del Gran Sasso, 67100 Assergi, Italy; stefano.pirro@lngs.infn.it
* Correspondence: marco.ricci@roma1.infn.it

Abstract: Cooling down large test masses up to 200 kg, as foreseen for the Einstein Telescope, is a complex challenge combining cutting-edge technological achievements from different disciplines with the experience gained from both room-temperature and cryogenic-temperature detector development communities. We set up an apparatus designed to test cryogenic mechanical suspensions for the payload system. They should have high quality factors and enable sufficient heat extraction greater than 0.3 W. The facility is on a university campus where cryofluid servicing is not feasible. As a result, a system that incorporates conductive cooling technology was developed. The project has two main goals: validating crystalline suspensions in a realistic Einstein Telescope cryogenic payload and testing new solutions for radiative thermal shielding. No particular measures are planned for the vibration isolation system.

Keywords: Einstein Telescope; gravitational wave detectors; cryogenics

check for updates

Academic Editor: Margo Aller

Received: 18 December 2024
Revised: 18 January 2025
Accepted: 7 February 2025
Published: 12 February 2025

Citation: Ricci, M.; Benedetti, E.; Cruciani, A.; Hoang, V.L.; Kalemi, B.; Naticchioni, L.; Orsini, M.; Pirro, S.; Puppo, P.; Rapagnani, P.; et al. Cryogenic Facility for Prototyping ET-LF Payloads Using Conductive Cooling. *Galaxies* **2025**, *13*, 12. https://doi.org/10.3390/galaxies13010012

Copyright: © 2025 by the authors. Licensee MDPI, Basel, Switzerland. This article is an open access article distributed under the terms and conditions of the Creative Commons Attribution (CC BY) license (https://creativecommons.org/licenses/by/4.0/).

1. Introduction

The Amaldi Research Center (ARC) was established at Sapienza University in Rome in 2018, named after the scientist who promoted the challenge of gravitational wave research in Italy. Later, thanks to European financial support (PNRR), the Einstein Telescope Infrastructure Consortium (ETIC) project was funded through a network of Italian institutions interested in the development of the Einstein Telescope. The proponent of the ETIC is the National Institute for Nuclear Physics, and the funding deadline is December 2025. By this date, all the infrastructure components must be constructed and delivered to the ARC; the assembly and subsequent test campaign will start from 2026. In this context, the activity hosted at Sapienza University, ARC-ETCRYO, was optimized to make the best use of the constraints imposed by the university campus logistics. One of them is related to the limited possibility of using large amounts of cryofluids, which are required for any ET-oriented activity. Indeed, experience from KAGRA teaches that Pulse-Tube-based cooling down with heat links is a valid solution for GW detectors of the second generation [1,2]. Rescaling to ET KAGRA cryogenics is not trivial; nonetheless, we optimized the scheme with some novel features and limited its functionality to real-sized cryogenic payload testing.

2. Cooling-Down Scheme

The baseline design of the ET-LF cryogenic payload features four different suspended stages: mirror, marionette (MA), platform (PF), and actuation cage (AC). Two alternative concepts have been proposed for heat extraction and the marionette suspension. The first concept relies on a cooling interface between the actuation cage and the platform, requiring a monocrystalline (silicon or sapphire) high-conductivity suspension for the marionette. The second concept uses a thin-wall titanium tube as a marionette suspension that is filled with superfluid He-II as outlined in [3]. The primary objective of the project is to validate the former cooling method (solid conduction) suspending a large test mass (TM), playing the role of the mirror, using high-quality-factor sapphire suspensions. The infrastructure is not compatible with the implementation of any realistic seismic isolation system due to limited room available in the lab. However, the KAGRA experience revealed the impact of other technical noise on the system, such as Pulse Tube (PT) operational vibrations, as in [4]. Soft thermal links and suspended parts are used in the system in order to limit the vibration injected into the system. The study of vibration attenuation by the refrigerators within the setup is one of the expected outcomes of the project [5].

The infrastructure consists of the following:

1. two refrigeration lines;
2. the cryostat C75;
3. the cryogenic payload.

Four PT cryocoolers are employed to cool down the setup. They will be located on the two refrigeration lines (see Figures 1 and 2), which will supply the cooling power to both the cryostat and the payload. In particular, one of the refrigeration lines is assigned to the cooling of the innermost radiation shield of the cryostat, while the other is entirely dedicated to the cooling of the payload. We remark that the label C75 was introduced to specify that the cryostat we are developing does not reach the full size (75%) envisaged for ET (estimated). However, the full-scale payload could in principle be tested. This is possible because we are limiting the purpose of the facility just to the payload development, and several features related to the seismic isolation system and to the interferometer are absent.

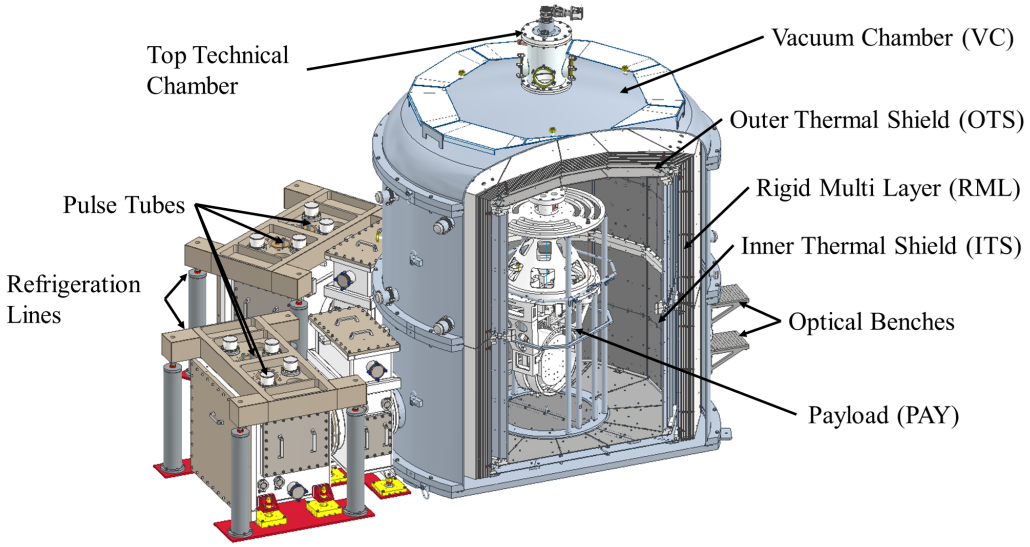

Figure 1. Sectional view of the ARC infrastructure. The cryostat houses the cryogenic payload, cooled by two refrigeration lines.

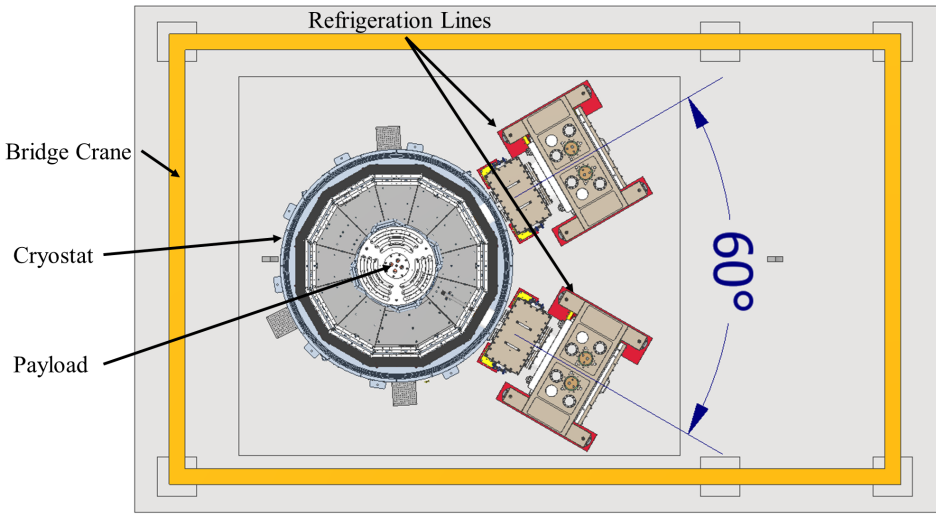

Figure 2. Top view of the ARC infrastructure inside the laboratory. The angle between the two refrigeration lines is shown.

3. Discussion

The sections of the apparatus are illustrated according to their functions, starting from the cooling system.

3.1. Refrigeration Lines

The cooling of the payload is performed through four Pulse Tube cryocoolers (Bluefors Syracuse, Syracuse, NY, USA) The refrigeration line accountable for the cooling of the cryostat shield will locate two Pulse Tube PT420 (certified performance 1.8 W@4.2 K with 50 W@45 K). The other refrigeration line will employ two Pulse Tube PT425 devices (certified performance 2.35 W@4.2 K with 50 W@45 K) [6]. These were chosen to cool down the payload because of their higher refrigeration power. These refrigerators were chosen since they lack moving parts at the cold end, making them ideal for low-vibration cryogenic experiments. However, they exhibit a vibrational peak at 1.4 Hz (with harmonics), clearly evident near the device. In order to reduce the impact of vibrations, PTs should be mechanically decoupled from the heat extraction path. This is the reason why we will employ soft heat links that are designed to mitigate vibrations but also thermally connect the system. Moreover, the two refrigeration lines were designed to locate the cryocoolers far from the cryostat and to damp the related vibrations.

To achieve this, each refrigeration line comprises two suspended stages: a cylindrical radiation shield thermally connected to the first stages of the PTs and a cold cooling bar connected to their second stages. A sectional view is shown in Figures 3 and 4. The radiation shield is constructed from aluminum series 1000, while the cooling bar is composed of aluminum 5N5 (99.9995 % purity).

High-purity materials, such as aluminum and copper, are adopted for thermal connections because of their excellent thermal conductivity at cryogenic temperatures and very low stiffness, which minimizes vibration transfer. The first-stage connection, between first stage of PT and the shield of the refrigeration line, is expected to be at 30 K. Thus, these soft heat links are composed of Oxygen-Free High-Conductivity (OFHC) copper braids characterized by peak thermal conductivity greater than 1500 W/m/K @30 K [7]. The second-stage connection, between the second stage of PT and the cooling bar, whose expected temperature is less than 10 K, comprises aluminum 6N (99.9999% purity) heat links composed of 12 thin foils, each 100 μm thick. This material exhibits an extremely high thermal conductivity peak, exceeding 10,000 W/m/K@10 K [8]. In order to monitor the

vibration attenuation, the refrigeration lines and the entire cryogenic infrastructure will include cryogenic sensors such as accelerometers and geophones.

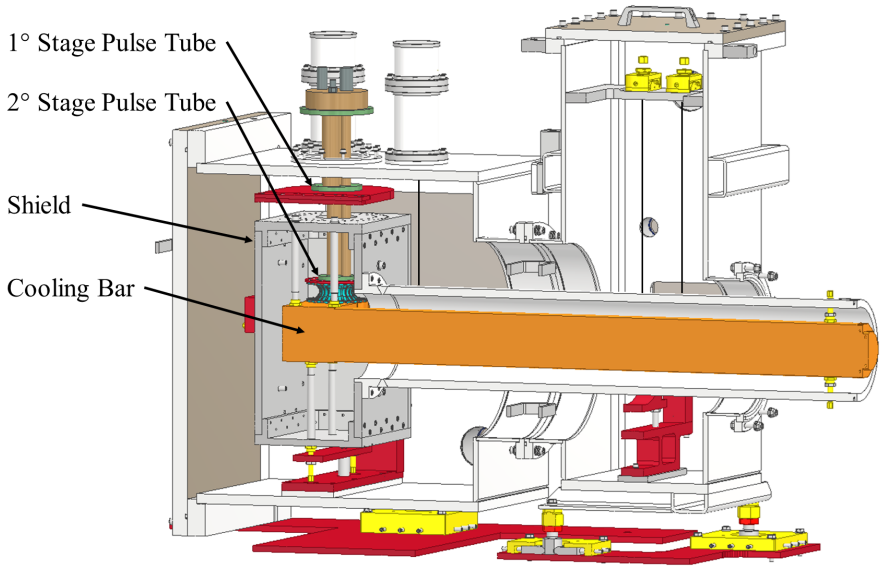

Figure 3. Sectional view of the refrigeration line. The orange component is the cooling bar connected to the second stages of the Pulse Tubes. The radiation shield surrounds the cooling bar, and it is connected to the first stages of the Pulse Tubes. Both of these components are suspended.

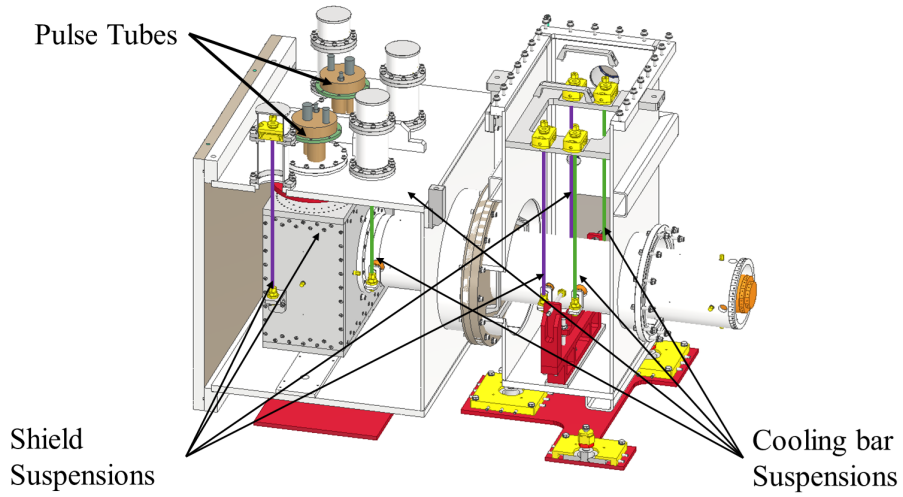

Figure 4. Sectional view of the refrigeration line. Suspensions of the shield and the cooling bar are highlighted. In green, the cooling bar suspension wires; in purple, the shield suspension wires.

3.2. Cryostat C75

The cryostat design must meet thermal requirements to enable the cooling of the payload to its target temperature. In particular, it consists of four main components (see Figure 1):

1. the vacuum chamber (VC), composed of Steel 304L. It is 2.95 m in diameter and 3.3 m in height. It comprises all the openings for optical levers, thermometer connections, both diode DT670 and Cernox ™(Lakeshore, Westerville, OH, USA), stiffeners, etc.;
2. the Outer Thermal Shield (OTS), composed of Al 6063. It has a dodecagonal shape, and its role is to shield the radiation coming from the room-temperature vacuum chamber. Its thermal insulation relies upon a novel thermal shield concept, Rigid Multi-Layer (RML);

3. the Inner Thermal Shield (ITS), composed of Al 6063. It has a dodecagonal shape and acts as a shield for the radiation emitted by the OTS to the payload. Moreover, it is exploited to help the cooling of the payload; hence, the inner surfaces are coated black in order to increase the emissivity and couple the cooling of the ITS to that of the payload;
4. the Top Technical Chamber (TTC). It contains the mechanism to suspend the payload and control its orientation once the C75 is closed. It is located on top of the vacuum chamber.

Since bottom access is not feasible due to room constriction, the VC, OTS, and ITS are horizontally divided into three main parts. This division enables access in the cryostat while only the bottom components are located in the laboratory in order to mount the payload and connect the heat links. Figure 5 shows the payload installation (and maintenance) configuration. The cryostat will then be assembled in whole with the middle horizontal components and closed with the dome. The payload will then be lifted and oriented through its suspension wire from the TTC.

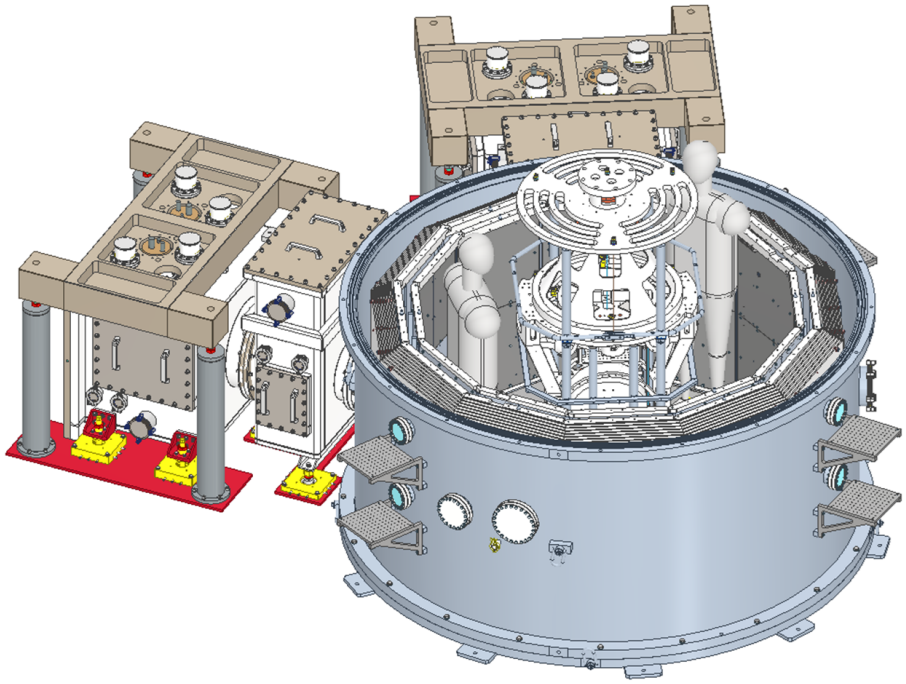

Figure 5. Payload installation and maintenance configuration of the cryostat.

The entire system has a single vacuum, which will be evacuated through two dry screw vacuum pumps and three turbomolecular pumps. In particular, a VARODRY VD65 (Leybold, Milan, Italy) and two TURBOVAC 350i (Leybold, Milan, Italy) will be used to pump the refrigeration lines, while a VARODRY VD100 and a MAG W 1300 iP (Leybold, Milan, Italy) are dedicated to the cryostat [9].

On the external surface of the VC, five optical benches are installed to allocate the optical lever, which will be used to monitor the payload angular motion, at the marionette and mirror levels (as shown in Figure 1).

The OTS is thermally connected to the radiation shields of both refrigeration lines with OFHC copper braids. The average target temperature of the OTS is 80 K; in order to reach such a temperature, a super-insulation system must be exploited. Typically, cryogenic systems adopt Mylar Multi-Layer Thermal insulation blankets to reduce the room temperature radiation due to the vacuum chamber. But, such a solution impacts the

timing of the overall vacuum-cooling process in order to avoid contamination and frost inside the cryostat.

Hence, we developed the Rigid Multi-Layer (RML) system, which consists of thin aluminum foils (thickness 0.3 mm) separated by insulating spacers and mounted on the external surfaces of the OTS. A number of 15 layers was chosen as a trade-off between heat load and mechanical issues (weight and installation). This leads to an expected heat flux on the external surfaces of the OTS of less than 1.6 W/m^2.

The ITS is connected to the cooling bar of one of the refrigeration lines via Al 6N foil-based heat links. Its average target temperature is 15 K. The black coating in its interior surfaces, which faces the payload, is exploited to boost the cooling of the payload through the radiation contribution, particularly during the initial cooling phase to approximately 120K. From this temperature to the target one, the radiation contribution becomes ineffective and the conduction contribution starts to be the dominant heat transfer method.

Both the OTS and ITS are propped up by hollow cylindrical supports, both on the edges of the bases and at the center, where the payload lies. Their shape is dodecagonal to ease the installation of the RML system and also to enable a perfect match between the refrigeration lines and the shields. There is an angle of 60° between the two refrigeration lines; therefore, a dodecagonal shape was chosen in order to enable the refrigeration lines to be perpendicular to the shield surfaces, as is evident in Figure 2. In order to increase the rigidity of the shields, stiffeners were implemented in the design. These are anchored on the VC surface and pull both the OTS and ITS from symmetrical points around the system (see Figure 1). On the other hand, in order to enable operators to work inside the cryostat, stiffening ribs are also installed beneath the base of the shields.

3.3. Cryogenic Payload

The payload (Figure 6) consists of a top platform, which is the first mass suspended by the TTC. From there, a sapphire rod is used to suspend the marionette. The mirror is suspended from the marionette using four sapphire ribbon-shaped suspensions, as is explained further in this Section. From the platform, three wires are used to suspend the actuation cage, which surrounds the marionette and the mirror. On the AC, several coils are mounted to move and actuate the mirror and the marionette while suspended; furthermore, it is equipped with PEEK stops, which act as a failsafe in case of failures and to assist with the mounting. The materials used for the components are Al 5083 (which shows a higher quality factor with respect to other aluminum series) and copper (which is mainly used to adjust the center of mass of the entire payload). The prototype has been developed with a dummy aluminum mirror (500 mm in diameter and 200 mm in thickness). In order to match the weight of its sapphire counterpart, several copper inserts have been envisaged in the body of the mirror. This enables the prototype and the entire facility to host a sapphire mirror in future tests maintaining the design. The mirror's target temperature is approximately 20 K, where sapphire exhibits a thermal conductivity peak over 10,000 W/m/K [10]. In ET-LF, this requirement enables extracting the heat absorbed by the TM due to the laser in the cavity and to avoid the formation of thermal gradients on the mirror surface. In the ARC prototype, the expected ET-LF heat input will be reproduced through heaters on the dummy aluminum mirror. In order to obtain the target temperature, the heat extraction path from the mirror to the cooling line should be well designed. In our scheme, the heat is extracted from the mirror via four sapphire ribbons, and then, from the marionette above, a sapphire rod will thermally connect the platform. Al 6N soft braids connect the platform to the AC and subsequently to the refrigeration line's cooling bar, ensuring efficient heat transfer.

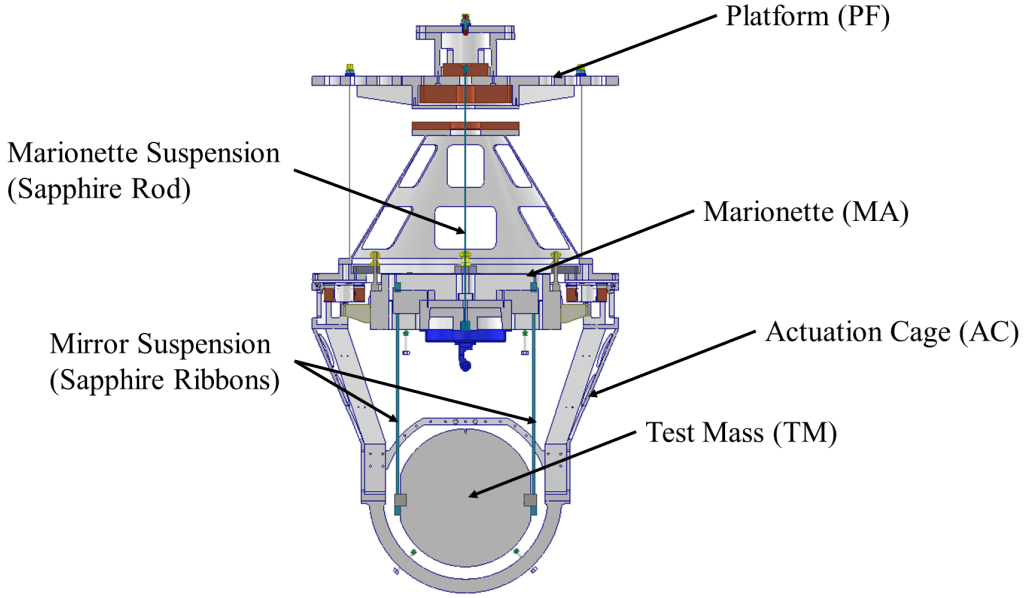

Figure 6. Section of the cryogenic payload to be installed into the cryostat. they first reach the actuation cage (AC) and then are connected to the sapphire solid conduction heat extraction path through the platform (PF).

Sapphire Suspensions

Although the current payload design includes a dummy mirror composed of aluminum and copper, the entire structure of the cryostat and payload is configured to enable the future suspension of a realistic crystalline TM. The ET collaboration is currently considering two different crystalline materials for the mirror and suspensions: sapphire and silicon. Both exhibit excellent thermal and mechanical properties at cryogenic temperatures. Since sapphire has a higher thermal conductivity than silicon, we are considering the former for the suspensions, although it is a material that is more challenging for companies to work with.

The suspension that connects the platform and the marionette is a sapphire rod of 5.4 mm in diameter and 760 mm in length. The rod is used to suspend the marionette with a mechanical mechanism of head clamping as shown in Figure 7.

A ribbon geometry solution was chosen for TM suspensions since it is potentially interesting for enhancing the dilution factor. As demonstrated in [11], dissipation dilution is greater by a factor of about 2 for rectangular crystalline silicon ribbons as compared to circular fibers at equivalent temperatures. The solution might also be explored for sapphire. The idea is to use Hydro-Catalysis Bonding (HCB) between two blocks of sapphire ($30 \times 20 \times 50$ mm) and two ribbons, shaped with a fillet meant to reduce the transversal degrees of freedom. Currently, preliminary tests of HCB-bonded suspension units have been performed on reduced-scale ribbons, 200 mm in length (see Figure 8). The initial shape adopted for the ribbons will be 1 mm thick, 7 mm wide, and 800 mm in length. The installation concept of the ribbon suspension unit enabled by this new design could prove to be very effective and innovative.

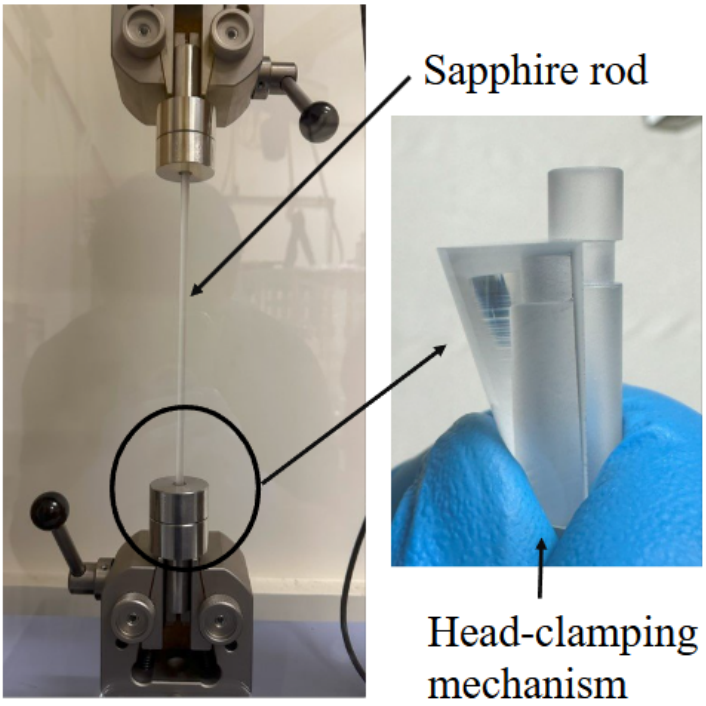

Figure 7. On the left is the sapphire rod designed to connect the platform and the marionette. On the right is a close-up view of the mechanical lock between the suspension rod and the platform/marionette. The lock utilizes a head-clamping mechanism.

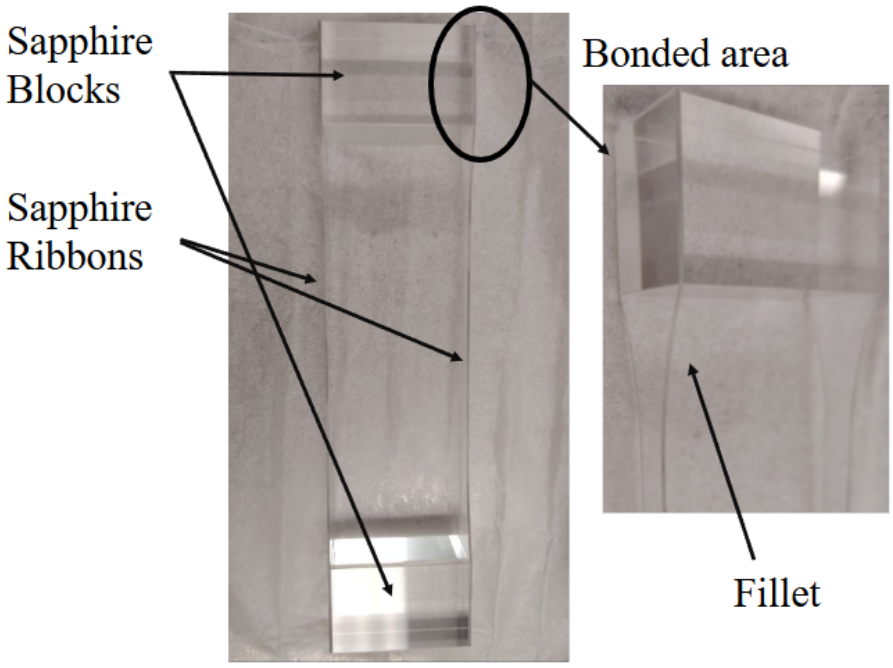

Figure 8. On the left is a reduced-scale ribbon suspension unit designed to connect the marionette with the test mass. It comprises two sapphire blocks bonded to two sapphire ribbons. On the right is a close-up view of the bonded region.

HCB is a high-precision bonding technique used in opto-mechanical systems and has already been implemented in the construction of quasi-monolithic silica suspensions in gravitational wave detectors. This type of chemical bonding can be performed using various aqueous solutions containing hydroxide ions to be applied at least on one of the

two bonding surfaces. A sodium silicate solution has been chosen for the HCB in our prototype suspension as it has been demonstrated that, comparatively, it offers the best strength properties among other solutions. For reliable bond formation with the HCB technique, the bonding surfaces must be flat. It has been shown that a flatness of $\leq \lambda/10$ ($\lambda = 633$ nm) is sufficient [12].

The prototype payload is designed to be flexible, enabling testing different shapes and designs of crystalline suspensions in the near future. For example, it can be modified from the current ribbon-shaped suspensions to a new system of fibers anchored to the crystalline ears of the mirror. Indeed, just very recently, promising results have been achieved at Glasgow through CO_2 welding on sapphire [13]; this technique might be considered later on. Furthermore, the system also allows changes to the suspension material, enabling testing the cryogenic payload with silicon instead of sapphire if necessary. This versatility ensures that our structure will be a testbed for various suspensions and mirrors in the future, facilitating the testing of different materials and designs to identify the best option for ET-LF purposes.

4. Simulations

Comprehensive thermal and structural simulations have been conducted to characterize the system's performance, primarily using ANSYS. Below, highlights of the main aspects simulated for the infrastructure are presented; a detailed description of these simulations will be provided in a dedicated paper currently in preparation.

- The steady-state temperature of the mirror: The target temperature of the mirror has been simulated considering the laser heat input (i.e., the heat input baseline of the ET-LF configuration) and all the heat input coming from the openings of the ITS (total of 0.3 W). The simulation result can be seen in Figure 9: the mirror steady-state temperature obtained is ∼15 K. This temperature is intentionally set lower than the target one in order to compensate for possible real effects, such as unpredictable heat loads and contact resistances in the heat links. In the simulation, the ITS temperature has been considered as the target one (15 K).

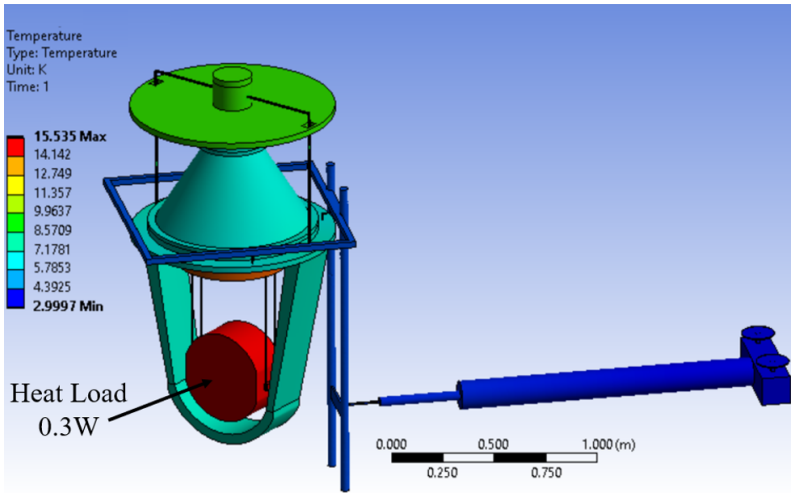

Figure 9. Results of steady-state thermal simulation of the payload considering the heat load (0.3 W) from the laser. The mirror temperature amounts to ∼15 K.

- The shielding efficiency of the RML System: Several solutions have been investigated to find an alternative solution to shield VC thermal radiation on the OTS. Eventually, the solution that minimizes the heat input on the OTS while maintaining rigidity and

cleanliness is the RML system. In order to validate the design, thermal and mechanical simulations have been performed.

Figure 10 shows the first eigenmode with an eigenfrequency value of 15.55 Hz, whilst the second and the third ones are 33.02 Hz and 55.85 Hz, respectively.

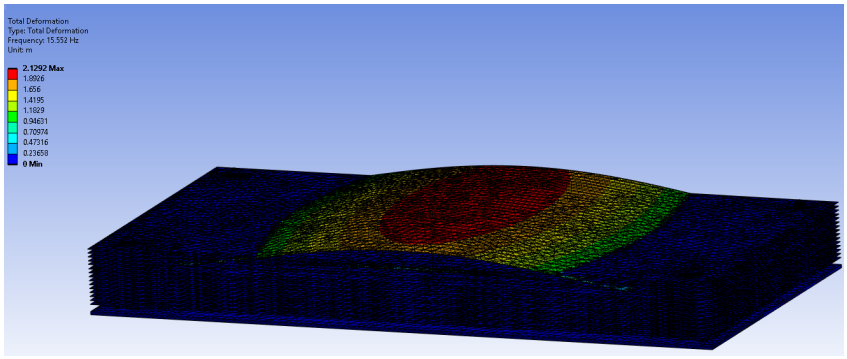

Figure 10. Results of modal simulations of the RML approach on one of the lateral surfaces of OTS. The figure shows the first eigenmode with its eigenfrequency value of 15.55 Hz.

Figure 11 shows the final temperature distribution along the RML system. The expected heat load on the OTS is 1.6 W/m^2 considering 15 layers of aluminum foil and a target temperature of OTS of 80 K.

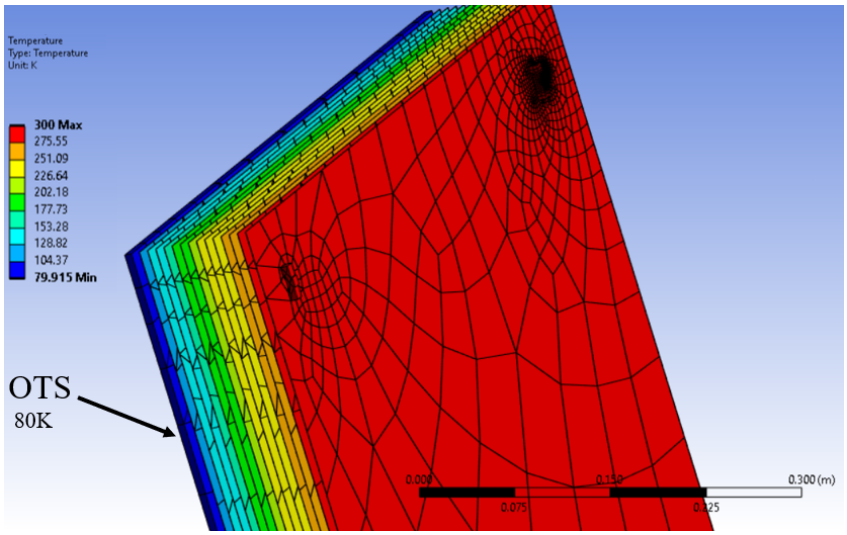

Figure 11. Results of steady-state thermal simulation of the RML approach on one of the lateral surfaces of OTS. A heat load of 1.6 W/m^2 resulted in 15 layers of RML and a target temperature of OTS of 80 K.

- Modal simulations: The structural modes of the whole structure have been analyzed in order to assess the validity within the ET constraints on frequencies. The results (see Figure 12) indicate the requirement of different stiffening elements: vertical and horizontal ones on the external surfaces of the OTS and ITS and stiffening rods to bind these to the VC. Hence, the first two eigenfrequencies increased from a value of around 15 Hz to 43 Hz.

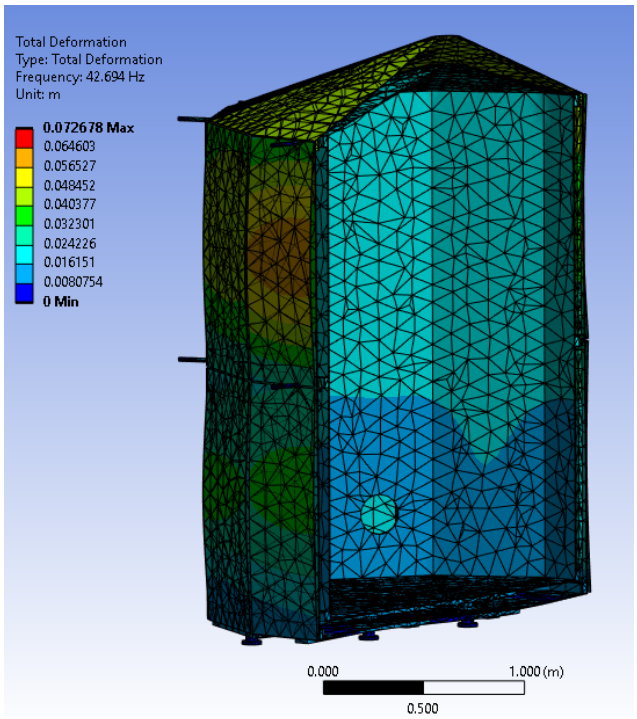

Figure 12. Results of modal simulations of the whole cryostat. Stiffeners can be observed installed on two different levels. RML geometry on each of the twelve surfaces has been simplified to ease the simulation. The figure shows the first eigenmode with its eigenfrequency value of 42.69 Hz.

5. Conclusions

The facility under development at the ARC-ETCRYO lab at Sapienza is dedicated to testing payload prototypes whose structures are not too far from the ET-LF baseline. Given the location and available room in the ARC-ETCRYO lab, the implementation of a seismic isolation system was not considered and the focus remains on cryogenic payload feasibility. A relevant part of the work concerning this activity is cryostat modeling concerning steady-state and transient conditions. The cryostat serves as the thermal connection between the payload and cooling devices located on the ground, similar to how the seismic isolation system acts as the mechanical connection to the ground. There are several issues related to cryogenic suspension and heat extraction that deserve further investigation in order to achieve a comparable state of knowledge.

Author Contributions: Conceptualization, L.N., P.P., P.R., F.R. and E.M.; Methodology, M.R. and P.P.; Software, M.R. and V.L.H.; Validation, M.R., E.B., A.C., V. L.H., B.K., M.O., S.P. and E.T.; Investigation, M.R., A.C., M.O. and S.P.; Writing—original draft, M.R., V.L.H. and B.K.; Supervision, E.M.; Funding acquisition, E.M. All authors have read and agreed to the published version of the manuscript.

Funding: The work reported in this contribution is supported by EC PNRR ETIC-IR0000004-Missione 4 and Italian PRIN LoVeC-ET 2020BSYXCB.

Data Availability Statement: Dataset available on request from the authors.

Acknowledgments: We thank N. Kimura at ICRR Univ. of Tokyo for the stimulating interaction concerning cryostat development, T. Yamada, KEK Tsukuba, for material characterization issues, and are indebted to Sheila Rowan, Glasgow Institute for Gravitational Wave Research, for sharing the HCB technology.

Conflicts of Interest: The authors declare no conflicts of interest.

Abbreviations

The following abbreviations are used in this manuscript:

ARC	Amaldi Research Center
ETIC	Einstein Telescope Infrastructure Consortium
ET	Einstein Telescope
KAGRA	Kamioka Gravitational Wave Detector
GW	Gravitational Wave
ET-LF	Einstein Telescope Low-Frequency
MA	Marionette
PF	Platform
AC	Actuation Cage
TM	Test Mass
PT	Pulse Tube
OFHC	Oxygen-Free High Thermal Conductivity
VC	Vacuum Chamber
OTS	Outer Thermal Shield
RML	Rigid Multi-Layer
ITS	Inner Thermal Shield
TTC	Top Technical Chamber
HCB	Hydro-Catalysis Bonding

References

1. Akutsu, T.; Ando, M.; Arai, K.; Arai, Y.; Araki, S.; Araya, A.; Aritomi, N.; Aso, Y.; Bae, S.W.; Bae, Y.B.; et al. Overview of KAGRA: Detector design and construction history. *Prog. Theor. Exp. Phys.* **2021**, *2021*, 05A101. [CrossRef]
2. Ushiba, T.; Akutsu, T.; Araki, S.; Bajpai, R.; Chen, D.; Craig, K.; Enomoto, Y.; Hagiwara, A.; Haino, S.; Inoue, Y.; et al. Cryogenic suspension design for a kilometer-scale gravitational-wave detector. *Class. Quantum Grav.* **2021**, *38*, 085013. [CrossRef]
3. Koroveshi, X.; Busch, L.; Majorana, E.; Puppo, P.; Rapagnani, P.; Ricci, F.; Ruggi, P.; Grohmann, S. Cryogenic payloads for the Einstein Telescope: Baseline design with heat extraction, suspension thermal noise modeling, and sensitivity analyses. *Phys. Rev. D* **2023**, *108*, 123009. [CrossRef]
4. Bajpai, R.; Tomaru, T.; Kimura, N.; Ushiba, T.;Yamamoto, K.; Suzuki, T.; Honda, T. Vibration analysis of KAGRA cryostat at cryogenic temperature. *Class. Quantum Grav.* **2022**, *39*, 165004. [CrossRef]
5. Yamada, T.; Tomaru, T.; Suzuki, T.; Ushiba, T.; Kimura, N.; Takada, S.; Inoue, Y.; Kajita, T. High performance thermal link with small spring constant for cryogenic applications. *Cryogenics* **2021**, *116*, 103280. [CrossRef]
6. Bluefors. Available online: https://bluefors.com/products/pulse-tube-cryocoolers/ (accessed on 15 December 2024).
7. Simon, N.J.; Drexler, E.S.; Reed, R.P. *Properties of Copper and Copper Alloys at Cryogenic Temperatures*; Final Report; NIST/MONO-177; National Institute of Standards and Technology (MSEL): Boulder, CO, USA, 1992.
8. Woodcraft, A.L. Recommended values for the thermal conductivity of aluminium of different purities in the cryogenic to room temperature range, and a comparison with copper. *Cryogenics* **2005**, *45*, 626–636. [CrossRef]
9. Leybold. Available online: https://www.leyboldproducts.it/ (accessed on 15 December 2024).
10. Touloukian, Y.S.; Powell, R.W.; Ho, C.Y.; Klemens, P.G. Volume 2. Thermal Conductivity-Nonmetallic Solids. In *Thermophysical Properties of Matter*; The TPRC Data Series; Tye, R.P., Ed.; Academic Press Inc.: New York, NY, USA, 1969.
11. Cumming, A.V.; Cunningham, L.; Hammond, G.D.; Haughian, K.; Hough, J.; Kroker, S.; Martin, I.W.; Nawrodt, R.; Rowan, S.; Schwarz, C.; et al. Silicon mirror suspensions for gravitational wave detectors. *Class. Quantum Grav.* **2014**, *31*, 025017. [CrossRef]
12. Douglas, R.; van Veggel, A.A.; Cunningham, L.; Haughian, K.; Hough, J.; Rowan, S. Cryogenic and room temperature strength of sapphire jointed by hydroxide-catalysis bonding. *Class. Quantum Grav.* **2014**, *31*, 045001. [CrossRef]
13. Docherty, J.; Cumming, A.; Callaghan, J.; Hammond, G. Laser welding of crystalline sapphire. In Proceedings of the 3rd Einstein Telescope Annual Meeting: Materials for Advanced Detectors 2024, Warsaw, Poland, 15 November 2024. Available online: https://indico.ego-gw.it/event/771/sessions/870/#20241115 (accessed on 16 November 2024).

Disclaimer/Publisher's Note: The statements, opinions and data contained in all publications are solely those of the individual author(s) and contributor(s) and not of MDPI and/or the editor(s). MDPI and/or the editor(s) disclaim responsibility for any injury to people or property resulting from any ideas, methods, instructions or products referred to in the content.